Analyzing the Tensile Behavior of Warp-Knitted Fabric-Reinforced Composites. Part II. Modeling the Tensile Modulus of Composite

Hadi Dabiryan*, Ali Asghar Asgharian Jeddi, and Mohammad Hossein Ashouri

Abstract- **In the first part of this series, a straight-line geometrical model was generated for Queen's Cord warp-knitted fabrics as reinforcement of the composite. In this part, the Rule of Mixture (ROM) was modified to calculate the elastic modulus of composites reinforced with Queen's Cord fabrics using the straight-line model. For this purpose, the geometrical model was divided into different segments, and their angle with the direction of applied force was obtained. Considering the alignment of each segment, the effective length of different segments of the unit-cell of fabrics was calculated. Using the effective length, an orientation coefficient was defined for tensile modulus of fibers in ROM. In order to evaluate the modified ROM, nine types of composites were fabricated using produced Queen's Cord fabrics. The results showed that modified ROM is closer to experiments than previous modifications.**

Keywords**: tensile modulus, rule of mixture, queen's cord, warp-knitted fabrics**

Nomenclature

l_{1f}, l_{2f}, l_{3f}	Length of segments in head of front bar loop
l_{1b}, l_{2b}, l_{3b}	Length of segments in head of back bar loop
l_{a1f}, l_{a2f}	Length of arms in front bar loop
l_{a1b}, l_{a2b}	Length of arms in back bar loop
α_f, β_f	Angles of front bar legs in plane
α_b, β_b	Angles of back bar legs in plane
E_{c1}	Young's modulus of composite in wale direction
E_{c2}	Young's modulus of composite in course direction
κ_c	Fiber modulus coefficient in course direction
κ_w	Fiber modulus coefficient in wale direction
d	Yarn diameter
l_{rf}	Length of roots in front bar
l_{rb}	Length of roots in back bar
w	Wale spacing
c	Course spacing
n_f	Number of underlaps for the front bar
n_b	Number of underlaps for the back bar
l_{uf}	Length of underlap in front bar loop
l_{ub}	Length of underlap in back bar loop
L_{tot}	Total length of the loop in the unit-cell

H. Dabiryan, A.A. Asgharian Jeddi, and M.H. Ashouri
Department of Textile Engineering, Amirkabir University of Technology, Tehran, Iran.

Correspondence should be addressed to H. Dabiryan
e-mail: dabiryan@aut.ac.ir

I. INTRODUCTION

It is common to use a micro-mechanics approach termed the Rule of Mixture (ROM) to predict composite stiffness. The application of ROM needs to assume that fibers are uniformly distributed throughout the matrix. Also, applied loads should be either parallel or normal to the fiber direction. When fabrics are used as reinforcement of composites, the made assumptions are not true. This fact confirmed that the ROM should be modified in fabric-reinforced composite applications. Tensile properties of fabric-reinforced composites have been investigated by many researchers [1-8]. Since the fibers in the structure of fabric are laid in the different directions, the tensile properties of fabric-reinforced composites do not follow the ROM. For this reason, the modification of ROM has been the subject of numerous researches [9-15]. Krenchel [9] initiated the modification of rule of mixture in fiber-reinforced composites. Based on the Krenchel's method, an efficient factor should be multiplied to Young's modulus of fibers in the rule of mixture to predict the Young's modulus of composite. Hearle *et al.* [16] defined the efficient factor considering the angle of fibers with load direction. Ramakrishna *et al.* [10] proposed a coefficient for the modulus of fibers in terms of proportion and the orientation of fiber bundle in the plain weft-knitted fabrics. Gommers *et al.* [11] considered architecture of loops in the structure of warp-knitted fabrics and defined a coefficient as length-weighted average of the fiber segments in the loop. Ghafaar *et al.* [12] studied the application of ROM to woven fabric-reinforced composites and found that the ROM equations give approximate upper bound values for all investigated composites. Huang [13] studied the mechanical properties of composites reinforced with woven and braided fabrics and defined a modified rule of mixture to predict the elastic properties of fabric composites under any arbitrary load condition. Virk *et al.* [14] defined a fiber area correction factor (FACF) to modify the ROM and generated a micromechanical model for the prediction of the tensile modulus of natural fiber-reinforced polymer matrix composites. Considering the noncircular cross-section of natural fibers, a new ROM was defined to provide a sensible estimate for the experimentally measured elastic modulus of the composite by Cullen *et al.* [15].

Literatures showed that the basic form of the ROM could not be used in the fabric-reinforced composites. In this paper, it is tried to find a coefficient to modify the ROM based on the effective length of segments in the straight-line model presented in the previous part [17].

II. EXPERIMENTAL

It is well known that the Young's modulus of fiber-reinforced composites (E_c) can be predicted using simple ROM as bellow:

$$E_c = E_f \nu_f + E_m \nu_m \tag{1}$$

Where, E_f is the Young's moduli of fiber, υ_f is the volume fraction of fiber, E_m is the Young's moduli of matrix, and υ_m is the volume fraction of matrix. When fabrics are used as reinforcement of composite, the ROM encounters with considerable error in predicting the Young's modulus of composites due to the different directions of fibers in the structure of fabric. In order to modify the ROM for fabric-reinforced composites, a coefficient is defined as ratio of effective length to the initial length of the unit-cell. For this purpose, the straight-line model generated for Queen's Cord fabrics is used as a case study. Figs. 1 and 2 show the different parts of front and back bar loops, respectively. Using the proposed model, the length of fibers in alignment of applied force is defined as the effective length.

Based on the geometrical equations derived for the unit-cell of Queen's Cord structures, the length of different straight parts of the front and back bar loops in the unit-cell is given by [17]:

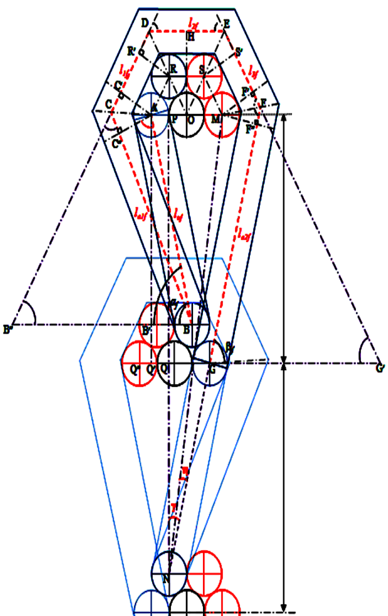

Fig. 1. Geometrical details of the front bar [17].

$$L = L_f + L_b \tag{2}$$

Where, L_f and L_b are the length of the front and back bar loops, respectively.

The length of front and back bar loops is obtained as follows:

$$L_f = L_{1f} + L_{2f} + L_{3f} + L_{a1f} + L_{a2f} + L_{uf} + L_{rf} \tag{3}$$

$$L_b = L_{1b} + L_{2b} + L_{3b} + L_{a1b} + L_{a2b} + L_{ub} + L_{rb} \tag{4}$$

The geometrical equations for calculating the length of different segments of front and back bar loops were derived [17]:

Front bar equations

$$\begin{cases} L_{1f} = \dfrac{d}{\tan\left(\dfrac{\alpha_f}{2}+\dfrac{\pi}{6}\right)} + d + \dfrac{d}{\sqrt{3}} \\ l_{2f} = 2.15d \\ l_{3f} = \dfrac{d}{\sqrt{3}} + d + \dfrac{d}{\tan\left(\dfrac{\beta_f}{2}+\dfrac{\pi}{6}\right)} \\ l_{uf} = \sqrt{\left(\tan\gamma.\left(c-\dfrac{\sqrt{3}}{2}.d\right)\right)^2 + \left(c-\dfrac{\sqrt{3}}{2}.d\right)^2} \\ l_{a1f} = \sqrt{l_{uf}^{\,2} - d^2} + \dfrac{d}{\tan\left(\dfrac{\alpha_f}{2}+\dfrac{\pi}{6}\right)} \\ l_{a2f} = \dfrac{d}{\tan\left(\dfrac{\beta_f}{2}+\dfrac{\pi}{6}\right)} + \dfrac{d}{\tan\eta} - \dfrac{\left(c-\dfrac{\sqrt{3}}{2}.d\right)}{\cos\gamma} \end{cases} \tag{5}$$

Where,

$$\alpha_f = \sin^{-1}\left(\frac{c-\frac{\sqrt{3}}{2}.d}{l_{uf}}\right) - \sin^{-1}\left(\frac{d}{l_{uf}}\right) \tag{6}$$

$$\beta_f = \frac{\pi}{2} - \gamma \tag{7}$$

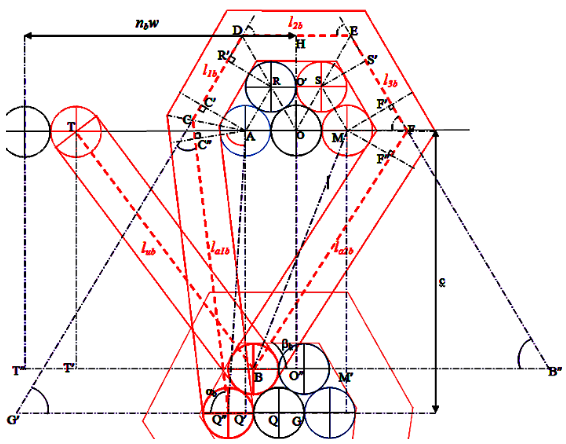

Fig. 2. Geometrical details of the back bar [17].

$$\eta = \sin^{-1}\left(\frac{d}{\sqrt{2.25d^2 + \left(2c - \frac{\sqrt{3}}{2}.d\right)^2}}\right) \tag{8}$$

Back bar equations:

$$\begin{cases} L_{1b} = \dfrac{d}{\tan\left(\dfrac{\alpha_b}{2}+\dfrac{\pi}{6}\right)} + d + \dfrac{d}{\sqrt{3}} \\ l_{2b} = 2.15d \\ l_{3b} = \dfrac{d}{\sqrt{3}} + d + \dfrac{d}{\tan\left(\dfrac{\beta_b}{2}+\dfrac{\pi}{6}\right)} \\ l_{ub} = \sqrt{\left(c - \dfrac{\sqrt{3}}{2}.d\right)^2 + [n_b w - 1.5d - Dev.]^2} \\ l_{a1b} = \sqrt{c^2 + dev.^2 - d^2} + \dfrac{d}{\tan\left(\dfrac{\alpha_b}{2}+\dfrac{\pi}{6}\right)} \\ l_{a2b} = \sqrt{\left(c - \dfrac{\sqrt{3}}{2}.d\right)^2 + (1.5d + Dev.)^2 - d^2} + \dfrac{d}{\tan\left(\dfrac{\beta_b}{2}+\dfrac{\pi}{6}\right)} \end{cases} \tag{9}$$

Where,

$$\alpha_b = \pi - \sin^{-1}\left(\frac{d}{\sqrt{c^2 + Dev.^2}}\right) - \tan^{-1}\left(\frac{c}{Dev.}\right) \tag{10}$$

$$\beta_b = \tan^{-1}\left(\frac{c - \frac{\sqrt{3}}{2}.d}{1.5d + Dev.}\right) - \sin^{-1}\left(\frac{d}{\sqrt{\left(c - \frac{\sqrt{3}}{2}.d\right)^2 + (1.5d + Dev.)^2}}\right) \tag{11}$$

$$Dev. = 1.5d - \tan\gamma.\left(c - \frac{\sqrt{3}}{2}.d\right) \tag{12}$$

$$\gamma = \tan^{-1}\left(\frac{1.5d}{2c - \frac{\sqrt{3}}{2}.d}\right) + \sin^{-1}\left(\frac{d}{\sqrt{2.25d^2 + \left(2c - \frac{\sqrt{3}}{2}.d\right)^2}}\right) \tag{13}$$

A. 3D State of the Model

In order to find the geometrical parameters of fabrics in 3D state, a straight-line model was proposed. The side view of 3D model is shown in Fig. 3.

The geometrical equations related to 3D model are as follows:

$$\Phi_{1f} = \tan^{-1}\left(\frac{d}{\frac{d}{\tan\left(\frac{\alpha_f}{2}+\frac{\pi}{6}\right)} + \frac{(1+\sqrt{3})d}{\sqrt{3}}}\right) \tag{14}$$

$$\Phi_{1b} = \tan^{-1}\left(\frac{d}{\frac{d}{\tan\left(\frac{\alpha_b}{2}+\frac{\pi}{6}\right)} + \frac{(1+\sqrt{3})d}{\sqrt{3}}}\right) \tag{15}$$

$$\Phi_{2f} = \tan^{-1}\left(\frac{2d}{\sqrt{\left(\left(2c - \frac{\sqrt{3}}{2}.d\right)^2 + 1.25d^2\right) + \frac{d}{\tan\left(\frac{\beta}{2}+\frac{\pi}{6}\right)}}}\right) \tag{16}$$

$$\Phi_{2b} = \sin^{-1}\left(\frac{\frac{\sqrt{3}}{2}d}{\frac{d}{\tan\left(\frac{\beta_b}{2}+\frac{\pi}{6}\right)} + \sqrt{\left(c - \frac{\sqrt{3}}{2}.d\right)^2 + (1.5d + Dev.)^2 - d^2}}\right) \tag{17}$$

Therefore, the Eqs. (3) and (4) become:

$$L_f = \frac{l_{1f}}{\cos\Phi_{1f}} + l_{2f} + \frac{l_{3f}}{\cos\Phi_{3f}} + l_{a1f} + \frac{l_{a2f}}{\cos\Phi_{2f}} + \frac{l_{uf}}{\cos\Phi_{2f}} + l_{rf} \tag{18}$$

$$L_b = \frac{l_{1b}}{\cos\Phi_{1b}} + l_{2b} + \frac{l_{3b}}{\cos\Phi_{3b}} + l_{a1b} + \frac{l_{a2b}}{\cos\Phi_{2b}} + l_{ub} + l_{rb} \tag{19}$$

According to the Krenchel's definition, the proposed coefficient (η) is given by [9]:

$$\eta = \frac{1}{L}\sum \cos^4(\alpha_i) l_i$$

Where, L is the total length of the loop, and α_i and l_i are the angle and length of each parts of the loops, respectively.

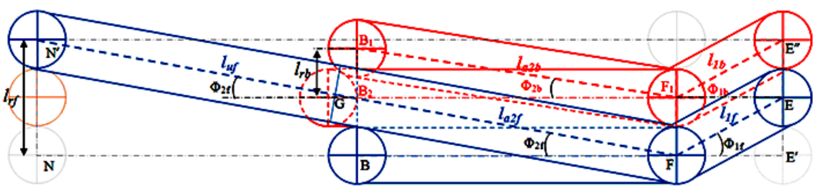

Fig. 3. Straight-line model for side view of the unit-cell [17].

Considering the straight-line model, the angle that each part forming with applied force direction is obtained. Using correspond angles, the effective length of each part in wale direction is calculated as follows:

Front bar equations

$$\begin{cases}(l_{1f})_{ew}=l_{1f}.\mathrm{Cos}(\alpha_1)\\(l_{2f})_{ew}=l_{2f}.\mathrm{Cos}(\alpha_2)\\(l_{3f})_{ew}=l_{3f}.\mathrm{Cos}(\alpha_3)\\(l_{uf})_{ew}=l_{uf}.\mathrm{Cos}(\frac{\pi}{2}-(\alpha_f+\delta))\\(l_{a1f})_{ew}=l_{a1f}.\mathrm{Cos}(\frac{\pi}{2}-\alpha_f)\\(l_{a2f})_{ew}=l_{a2f}.\mathrm{Cos}(\frac{\pi}{2}-\beta_f)\end{cases}\qquad(20)$$

Back bar equations

$$\begin{cases}(l_{1b})_{ew}=l_{1b}.\mathrm{Cos}(\alpha_1)\\(l_{2b})_{ew}=l_{2b}.\mathrm{Cos}(\alpha_2)\\(l_{3b})_{ew}=l_{3b}.\mathrm{Cos}(\alpha_3)\\(l_{ub})_{ew}=c-\frac{\sqrt{3}}{2}d\\(l_{a1b})_{ew}=l_{a1b}.\mathrm{Cos}(\frac{\pi}{2}-\alpha_b)\\(l_{a2b})_{ew}=l_{a2b}.\mathrm{Cos}(\frac{\pi}{2}-\beta_b)\end{cases}\qquad(21)$$

Similarly, the effective length of each part in course direction is calculated as follows:

Front bar segments

$$\begin{cases}(l_{1f})_{ec}=l_{1f}.\mathrm{Cos}(\frac{\pi}{2}-\alpha_1)\\(l_{2f})_{ec}=l_{2f}.\mathrm{Cos}(\frac{\pi}{2}-\alpha_2)\\(l_{3f})_{ec}=l_{3f}.\mathrm{Cos}(\frac{\pi}{2}-\alpha_3)\\(l_{uf})_{ec}=l_{uf}.\mathrm{Cos}(\alpha_f+\delta)\\(l_{a1f})_{ec}=l_{a1f}.\mathrm{Cos}(\alpha_f)\\(l_{a2f})_{ec}=l_{a2f}.\mathrm{Cos}(\beta_f)\end{cases}\qquad(22)$$

Back bar segments

$$\begin{cases}(l_{1b})_{ec}=l_{1b}.\mathrm{Cos}(\frac{\pi}{2}-\alpha_1)\\(l_{2b})_{ec}=l_{2b}.\mathrm{Cos}(\frac{\pi}{2}-\alpha_2)\\(l_{3b})_{3c}=l_{ab}.\mathrm{Cos}(\frac{\pi}{2}-\alpha_3)\\(l_{ub})_{ec}=n_b w-1.5d-\mathrm{Dev.}\\(l_{a1b})_{ec}=l_{a1b}.\mathrm{Cos}(\alpha_b)\\(l_{a2b})_{ec}=l_{a2b}.\mathrm{Cos}(\beta_b)\end{cases}\qquad(23)$$

Therefore, the effective length of front and back bar loops in the wale and course directions is equal:

$$(L_f)_{ew}=(l_{1f})_{ew}+(l_{2f})_{ew}+(l_{3f})_{ew}+(l_{a1f})_{ew}+(l_{a2f})_{ew}+(l_{uf})_{ew}+l_{rf}\qquad(24)$$

$$(L_b)_{ew}=(l_{1b})_{ew}+(l_{2b})_{ew}+(l_{3b})_{ew}+(l_{a1b})_{ew}+(l_{a2b})_{ew}+(l_{ub})_{ew}+l_{rb}\qquad(25)$$

The total effective length in the wale direction is:

$$(L_{tot.})_{ew}=(L_f)_{ew}+(L_b)_{ew}\qquad(26)$$

Consequently, the coefficient of fiber modulus in the wale direction is defined as bellow:

$$\kappa_w=\frac{(L_{tot.})_{ew}}{L_{tot.}}\qquad(27)$$

Using κ_w, the ROM is modified as follows:

$$E_{c1}=\kappa_w E_f \nu_f+E_m\nu_m\qquad(28)$$

Similarly, the effective length of front and back bar loops in the course directions would be:

$$(L_f)_{ec}=(l_{1f})_{ec}+(l_{2f})_{ec}+(l_{3f})_{ec}+(l_{a1f})_{ec}+(l_{a2f})_{ec}+(l_{uf})_{ec}+l_{rf}\qquad(29)$$

$$(L_b)_{ec}=(l_{1b})_{ec}+(l_{2b})_{ec}+(l_{3b})_{ec}+(l_{a1b})_{ec}+(l_{a2b})_{ec}+(l_{ub})_{ec}+l_{rb}\qquad(30)$$

Hence, the total effective length of loops in the course direction is:

$$(L_{tot.})_{ec}=(L_f)_{ec}+(L_b)_{ec}\qquad(31)$$

Therefore, the coefficient of fiber modulus in the course direction becomes:

$$\kappa_c=\frac{(L_{tot.})_{ec}}{L_{tot.}}\qquad(32)$$

Consequently, the composite modulus in the course direction is modified as bellow:

$$E_{c2}=\kappa_c E_f \nu_f+E_m\nu_m\qquad(33)$$

III. RESULTS AND DISCUSSION

A. Verification of the Model

Warp-knitted reinforced composites were fabricated using nine types of polyester Queen's Cord fabrics in order to check the accuracy of the modified ROM. The details of used fabrics are presented in Table I. The epoxy resin model ML506 and hardener HA-11 were used to produce composites by hand lay-up method. As shown in Fig. 4, the tensile test was carried out on the prepared samples using the INSTRON (Model: 5566) tensile tester with jaw speed of 2 mm/min, gage length of 170 mm and width of 25 mm according to ASTM D3093-76.

The fiber modulus coefficients in the wale and course directions (κ_w, κ_c) were calculated for all types of fabrics using the geometrical parameters of fabrics shown in Table I

TABLE I
CHARACTERISTICS OF POLYESTER QUEEEN'S CORD FABRICS

Level of density	Sample code	Number of underlaps		CPC	WPC	Fabric mass (g/m^2)
		FB	BB			
Loose	Q2l	1	2	12.6	11.9	98.12
Medium	Q2m	1	2	19.4	12.1	126.1
Tight	Q2t	1	2	23.3	11.8	137.5
Loose	Q3l	1	3	12.1	11.6	106.3
Medium	Q3m	1	3	17.3	11.8	128.6
Tight	Q3t	1	3	22.9	11.6	146
Loose	Q4l	1	4	11.8	11.8	116.6
Medium	Q4m	1	4	17.4	11.8	145.6
Tight	Q4t	1	4	22.8	11.8	163.6

TABLE II
FIBER MODULUS COEFFICIENTS

Sample code	Krenchel's coefficients		Suggested coefficients	
	κ_w	κ_c	κ_w	κ_c
Q2l	0.5695	0.2275	0.7252	0.4353
Q2m	0.4364	0.3311	0.6148	0.5450
Q2t	0.3743	0.3844	0.5595	0.5931
Q3l	0.51438	0.3222	0.6585	0.4922
Q3m	0.4110	0.4066	0.5645	0.5812
Q3t	0.32450	0.4784	0.4845	0.6496
Q4l	0.4747	0.3864	0.6078	0.5331
Q4m	0.3635	0.4802	0.5014	0.6300
Q4t	0.2879	0.5416	0.4303	0.6896

and related equations. The calculated coefficients are presented in Table II.

The mechanical properties of polyester fibers and epoxy resin are listed in Table III.

The relation between the experimental and theoretical tensile modulus based on the Krenchel's modification is shown in Fig. 5. As can be seen, in both wale and course directions, the experimental values are greater than theoretical values. Also, except from Q2l sample, there is a considerable difference between the theoretical and experimental results. The Krenchel's model does not consider the 3D state of the geometry of the unit-cell. Therefore, the calculated total length of the fibers in the unit-cell is less than the real length. It leads to reduce the volume fraction of fibers in the composite, considerably.

TABLE III
MECHANICAL PROPERTIES OF CONSTITUENT OF COMPOSITES

PET fibers		Epoxy resin (ML-506)	
E_f (MPa)	7	E_m (GPa)	682
ν_f (%)	0.33	ν_m (%)	0.67

Fig. 4. Instron tensile tester for testing of composites.

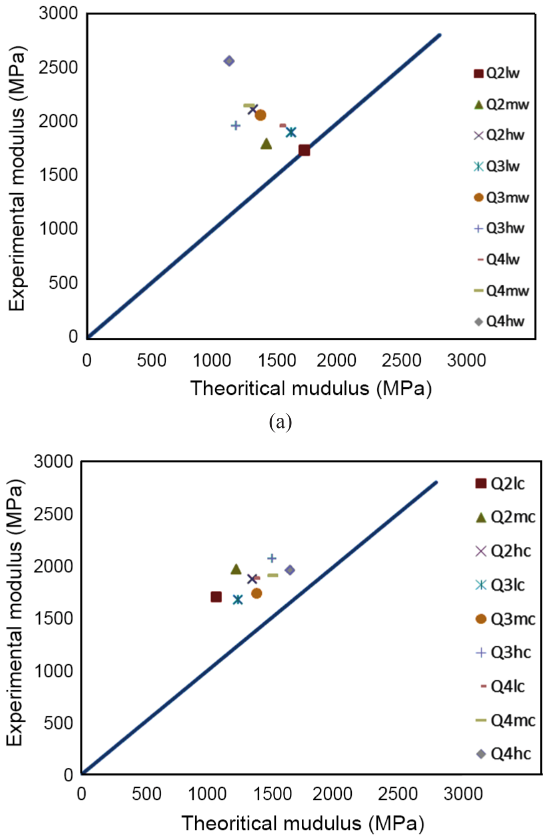

Fig. 5. Comparison between experimental modulus and theoretical tensile modulus based on Krenchel's coefficient: (a) wale direction and (b) course direction.

Fig. 6 shows the relation between the experimental and theoretical elastic modulus based on the proposed coefficient to modify the ROM. As seen in Fig. 6a, except from Q4h sample, there is a reasonable agreement between the experimental and theoretical tensile modulus. While, there is a quite agreement between the theoretical and experimental results in course direction (Fig. 6b).

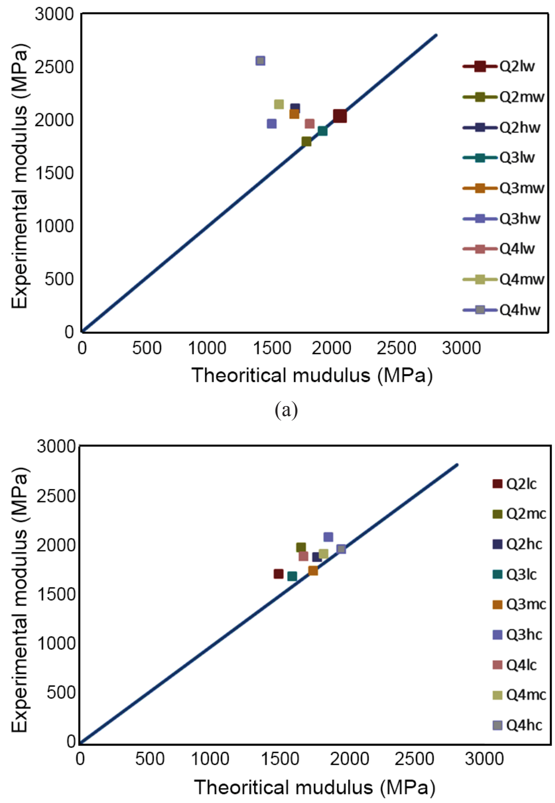

Fig. 6. Comparison between experimental modulus and theoretical tensile modulus based on suggested coefficient: (a) wale direction and (b) course direction.

Comparison between points by points of Figs. 5 and 6 confirms that in both wale and course directions, the results of proposed coefficient are closer to the experiments than Krenchels's coefficient.

The differences between the experimental and theoretical results of models directions are presented as error percentage of wale and course directions in Tables IV and V, respectively. As shown, in all cases the results of the

TABLE IV
COMPARISON BETWEEN THEORETICAL AND EXPERIMENTAL TENSILE MODULUS IN WALE DIRECTION

Sample's code	Experimental results	Krenchel's model		Presented model	
		Theoretical results	Err. (%)	Theoretical results	Err. (%)
Q2lw	2034.7	1736.0	14.7	2044.3	-0.5
Q2mw	1793.2	1428.3	20.4	1781.5	0.6
Q2tw	2109.1	1325.4	37.2	1692.1	19.8
Q3lw	1895.1	1623.7	14.3	1909.1	-0.7
Q3mw	2055.5	1383.2	32.7	1687.3	17.9
Q3tw	1961.4	1191.0	39.3	1507.8	23.1
Q4lw	1962.5	1544.2	21.3	1807.8	7.9
Q4mw	2142.8	1294.2	39.6	1567.3	26.9
Q4tw	2554.2	1138.6	55.4	1420.7	44.4

TABLE V
COMPARISON BETWEEN THEORETICAL AND EXPERIMENTAL TENSILE MODULUS IN COURSE DIRECTION

Sample's code	Experimental results	Krenchel's model		Presented model	
		Theoretical results	Err. (%)	Theoretical results	Err. (%)
Q2lc	1069.9	1697.9	37.0	1481.3	12.8
Q2mc	1227.0	1965.8	37.6	1650.5	16.0
Q2tc	1355.4	1867.2	27.4	1768.8	5.3
Q3lc	1243.2	1676.2	25.8	1579.8	5.7
Q3mc	1392.5	1737.1	19.8	1738.2	-0.1
Q3tc	1510.1	2070.9	27.1	1849.2	10.7
Q4lc	1372.7	1880.4	27.0	1663.2	11.6
Q4mc	1515.3	1905.7	20.5	1811.8	4.9
Q4tc	1653.8	1952.1	15.3	1947.0	0.3

generated model are closer to the experimental results than Krenchel's model.

IV. CONCLUSION

When the fabrics are used as the reinforcements of composites, the ROM needs to modify for calculating the composite stiffness due to orientation of fibers in the structure of fabrics. If a knitted-fabric is subjected to the tensile loads in wale or course direction, fibers in the structure of unit-cell make angles with direction of applied loads. Therefore, the ROM should be modified to predict the tensile modulus of fabric-reinforced composites. The Krenchel's modification is based on the angle of fibers direction with applied load in the fiber-reinforced composite. Considering the generated straight-line model for the structure of warp-knitted fabrics, modification coefficients are proposed to the fiber modulus in the ROM. The results showed that the modified ROM has a good agreement with experimental results of tensile modulus of composites in both wale and course directions. Also, the comparison between the results of different modified ROMs confirmed that the results of proposed model are closer to the experiments than Krenchel's modification.

REFERENCES

[1] P. Xue, J. Cao, and J. Chen, "Integrated micro/macro-mechanical model of woven fabric composites under large deformation", *Compos. Struct.*, vol. 70, pp. 69–80, 2005.

[2] Y. Miao, E. Zhou, Y. Wang, and B.A. Cheeseman, "Mechanics of textile composites: micro-geometry", *Compos. Sci. Technol*., vol. 68, pp. 1671–1678, 2008.

[3] K.H. Leong, S. Ramakrishna, Z.M. Huang, and G.A. Bibo, "The potential of knitting for engineering composites", *Composites: Part A*, vol. 31, 197–220, 2000.

[4] W.L. Wu, M. Kotaki, and A. Fujita, "Mechanical properties of warp-knitted, fabric-reinforced composites", *J. Reinf. Plast. Comp*., vol. 12, pp. 1096-1110, 1993.

[5] Z.M. Huang, S. Ramakrishna, and A.A.O. Tay, "A micromechanical approach to the tensile strength of a knitted fabric composite", *J. Compos. Mater.*, vol. 33, pp. 1758-1791, 1999.

[6] Z.M. Huang, S. Ramakrishna, and A.A.O. Tay, "A unified micromechanical model for estimating elastic, elasto-plastic, and strength behaviors of knitted fabric reinforced composites", *J. Reinf. Plast. Comp.*, vol. 19, pp. 642-656, 2000.

[7] N.K. Nail and V.K. Ganesh, "Prediction of on-axes elastic properties of plain weave fabric composites", *Comp. Sci. Tech.*, vol. 45, pp. 135-152, 1992.

[8] N.G. Andre and Z.A. Mohd. Ishak, "Predicting the tensile modulus of randomly oriented nonwoven kenaf/epoxy composites", *Procedia Chem.*, vol. 19, pp. 419-425, 2016.

[9] H. Krenchel, Fibre Reinforcement, Akademisk Forlag, Copenhagen, 1964.

[10] S. Ramakrishna, N.K. Cuong, and H. Hamada, "Tensile properties of plain weft knitted glass fiber fabric reinforced epoxy composites", *J. Reinf. Plast. Comp.*, vol. 16, pp. 946-966, 1997.

[11] B. Gommers, I. Verpoest, and P. Van Houtte, "1996 modelling the elastic properties of knitted-fabric-reinforced composites", *Compos. Sci. Technol.*, vol. 56, pp. 685-694, 1996.

[12] M.A. Ghafaar, A.A. Mazen, and N.A. El-Mahallawy, "Application of the rule of mixtures and Halpin-Tsai equations to woven fabric reinforced Epoxy

composites", *J. Eng. Sci.*, vol. 34, no. 1, pp. 227-236, 2006.

[14] A.S. Virk, W. Hall, and J. Summerscales, "Modulus and strength prediction for natural fibre composites", *Mater. Sci. Technol.*, vol. 28, pp. 864-871, 2012 .

[15] J.W. Hearle, J.J. Thwaites, and J. Amirbayat, "Mechanics of flexible fibre assemblies", *Nato Adv. Stud. Inst. Se. E: Appl. Sci*., 1980.

[16] R.K. Cullen, M.M. Singh, J. Summerscales, "Characterisation of natural fibre reinforcements and composites", *J. Compos.*, vol. 2013, pp. 1-4, Article ID 41650, 2013.

[17] H. Dabiryan and A.A.A. Jeddi, "Analyzing the tensile behavior of warp-knitted fabric reinforced composites, part I: modeling the geometry of reinforcement", *J. Text. Polym.*, vol. 4, no. 2, pp. 68-74, 2016.